TOPOLOGY OPTIMIZATION OF COMPLIANT MECHANISMS AS A DESIGN METHOD TO IMPROVE HARDWARE PERFORMANCE IN LUNAR DUST ENVIRONMENT

Dorota Budzyń [(1)], Hossein Zare-Behtash [(2)], Aidan Cowley [(3)], Andrea Cammarano [(4)]

[(1)] University of Glasgow, Glasgow, Scotland, G12 8QQ, United Kingdom, d.budzyn.1@research.gla.ac.uk
[(2)] University of Glasgow, Glasgow, Scotland, G12 8QQ, United Kingdom, hossein.zare-behtash@glasgow.ac.uk
[(3)] European Space Agency, European Astronaut Centre, Linder Höhe, Cologne 51147, Germany, aidan.cowley@esa.int
[(4)] University of Glasgow, Glasgow, Scotland, G12 8QQ, United Kingdom, andrea.cammarano@glasgow.ac.uk

1. ABSTRACT

The experience from the Apollo missions showed that Lunar regolith particles are exceptionally sharp, electrostatically charged, adhesive, and pose a significant risk to mission hardware by entering gaps between the elements of mechanisms and can cause damage especially where rigid body relative displacements occur. The present work presents an alternative approach for the design of hardware that will operate on the Lunar surface. The authors propose the use of compliant mechanisms to produce monolithic mechanisms that are intrinsically resilient to Lunar dust. To support the design of compliant mechanisms topology-optimisation based design methods are here proposed.
Topology optimization focuses on optimizing material distribution for a given design space and boundary conditions with the goal of maximizing the performance of the design.
Achieving topologically optimized compliant mechanisms, so far, has proven to be challenging, especially when compared to static structures, and the use of commercial software does not automatically translate in ease of use. In this work, several MATLAB routines that can support topology optimisation of compliant mechanisms are explored. The advantages and disadvantages of each routine are highlighted and their application to a compliant force inverter is presented.

2. LUNAR DUST ENVIRONMENT

The surface of the Moon is covered with debris and dust that have very sharp edges which have been created by numerous meteorite impacts (Lunar meteoric gardening) [1]. Not being exposed to the erosive environment present on Earth - e.g. hydrological and aeolian processes - the regolith fines remain sharp and abrasive. The size of these fine Lunar dust particles is less than 34µm and during the Apollo program particles smaller than 2µm proved to be the most problematic [2]. The smallest particles can enter gaps, clearances and backlashes that are exposed to this dusty environment. After penetrating the hardware gaps, the dust can jam the rigid body mechanisms which are key elements of most of the hardware. Because of this, Lunar dust poses a threat to sustainable surface operations and dust mitigation is a critical a critical exploration technology [3], [4].
Lunar dust contamination in long-duration missions may be difficult to avoid as the dust can float above the surface in a levitation like manner due to the electrostatic phenomena [5]. As the literature shows [6], the gravity force has a higher value than the opposing electrostatic one and the dust falls slowly to the ground. However, the consequence is that the dust can easily float above the ground and cover the surfaces of equipment especially in the terminator regions - during sunset and sunrise. The electrostatic charge of the Lunar surface is caused by multiple environmental factors. The day side of the Moon is hit by a solar wind of plasma electrons, ions and solar UV rays which cause photoemission [1], [7]. This is briefly presented in the Figure 1. The result of this phenomena is the positive charge of the dayside of the Moon with the plasma sheath containing photoelectrons above the surface. The sheath on the day side extends to roughly 1 m. On the night side of the Moon the negative charge develops and the "Debye sheath", dominated by positive ions, can extend from meters to even 1 km above the surface [8]. The surface charge can go up to +3 V on the day side and -200 V on the night side [9].

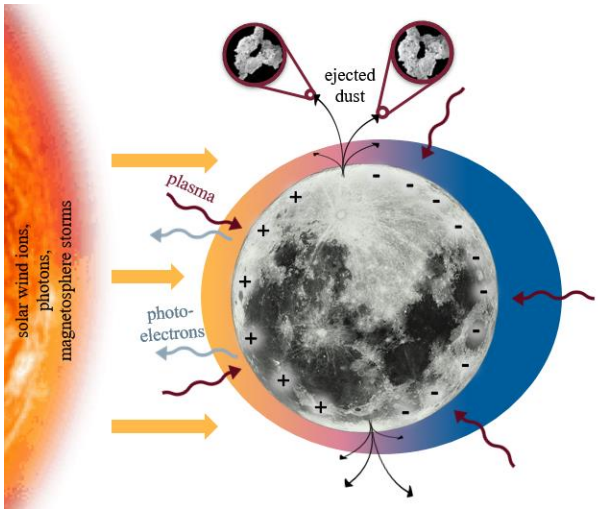

Figure 1. Lunar dust ejection mechanisms. Sheath colours: yellow – "photoelectron sheath", blue "Debye sheath", pink terminator areas.

All mentioned surface phenomena depend on solar activity and therefore are hard to account for in the specific moment of the mission. The resulting electrostatic charge has a different value depending on the work function of the local materials. The hardware surfaces, having a work function different than that of the regolith particles, will acquire a different electrostatic potential than the dust particles. Compared to van der Waals forces, the electrostatic potential difference has a higher impact on the adhesion of Lunar dust particles to hardware surfaces [5].

During the Apollo 17 Technical Crew Debriefing [2] on January 4, 1973, astronaut Gene Cernan stated: "*Close to the end of the third EVA, all the mechanical devices on the gate and on the pallet in terms of bag holders and pallet locks and what have you were to the point that they would refuse to function mechanically even though the tolerances on these particular locks were very gross. They didn't work because they were inhabited and infiltrated with this dust. Some could be forced over centre. Others just refused to operate even after dusting, cleaning, and a slight amount of pounding trying to break the dust loose. I think dust is probably one of our greatest inhibitors to a nominal operation on the Moon. I think we can overcome other physiological or physical or mechanical problems except dust."* This opinion is based on Cernan's experience from extravehicular activities on the Moon and the dust related problems that he experienced and that will be further discussed in the next section.

3. APOLLO HARDWARE PROBLEMS

Dust related problems identified during the Apollo surface missions have been classified into following categories [2]:

1. vision obscuration
2. false instrument readings
3. dust coating and contamination
4. loss of traction
5. clogging of mechanisms
6. abrasion
7. thermal control problems
8. seal failures
9. inhalation and irritation

In this work we mainly focus on clogging of the mechanisms. Other problems such as dust coating and contamination, abrasion and seal failures are related to this issue and therefore will also be discussed.

Apollo surface hardware interactions with dust particles led to several instances of damage [2]. The list includes: scratches on numerous optical instruments, damage to the fabrics of space suits, scratches of thermal coatings and jamming of moving parts and mechanisms in the scientific hardware. Protecting equipment from the Lunar dust is more challenging compared to Earth dust protection. As discussed earlier, the electrostatic phenomena and solar activity can cause dust to float above the Lunar surface. The reduced gravity and a lack of atmosphere complicate the issue even further by enabling the ejected dust particles to come back to the surface at slower speeds, which extends their residence time off the ground. Once electrostatically charged particles cover the surfaces of the hardware it is difficult to remove them. Apollo astronauts tried using brushes to remove dust from certain instruments. This was ineffective, and they only managed to drag the dust around without fully loosening its contact with the surfaces. This means that both protecting and cleaning the hardware poses a challenge. Scientists and engineers around the world are looking into new ways of protecting equipment from the Lunar dust. Several research topics focus on coatings as passive dust protection measures: nanostructured coatings reducing Van der Waals forces, peel off coatings and electrostatic discharge films [5]. Alternatively, active methods are also under investigation, such as: brushing, blowing, vibrating, and ultrasonic-driven techniques [5]. The main difference is that active methods require energy during operations. A typical passive method of protecting moving parts from getting jammed with a sand or dust is to seal them off from the dust-laden environment. Common methods for protection include labyrinths, rubber seals etc. These methods, however, rarely ensure full elimination of particles entering the assembly. They delay and minimize the contamination rather than eliminate it indefinitely. This is a good solution when maintenance is acceptable, or the operations of the equipment are quite short compared to the time it takes the contaminant to enter the assembly. This might not be enough for longer Lunar missions, and we propose to avoid hinge usage at the design level. To support the kinematic requirements, we propose to use friction-free solutions – compliant mechanisms.

4. FROM CLASSICAL SOLUTIONS TO COMPLIANT MECHANISMS

Compliant mechanisms are often designed as monolithic pieces that fulfil their kinematic function by elastic deformation [10]. This gives the possibility to reduce the mass and component count. Input work is converted into elastic energy and deflection fulfils the desired kinematic function. There is no relative motion of components and no friction as the mechanism is one deformable component – see for example Figure 2.

Figure 2. Compliant butterfly hinge.

For the mentioned reasons compliant mechanisms have been already recognized as solutions for precision engineering [11]–[13]. The fact that they are friction-free

solutions whose function cannot be impacted by dust contamination makes them ideal candidates to be used in the Lunar environment.

Designing compliant mechanisms can be unintuitive and requires some additional creative effort. Different approaches to the design method are listed in Figure 3.

Frequently used design methods for compliant mechanisms are analytical methods with the most popular being the Rigid Body Replacement Method [14]. This method helps to redesign existing rigid body solutions (traditional mechanisms) into compliant ones by replacing rigid kinematic pairs with flexures. The flexures are thin areas of the material that enable extensive deflection and support the desired kinematic behaviour. An example of such a replacement is visible in the Figure 4.

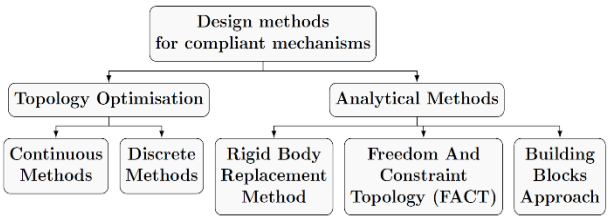

Figure 3. Different methods of designing compliant mechanisms.

The biggest disadvantage of this approach is the fact that it starts with a rigid body design and therefore the final topology will resample the rigid body solution which often is not the optimum material layout from a stress distribution point of view. Another downside is the fact that typically hinges are replaced with flexures. As mentioned, they are thin elements that deflect supporting the motion. When very localised, flexures are referred to as de-facto hinges [15]– this is due to the fact that such designs will have stiff structure-like areas and thin flexures behave like hinges. Those flexures are also the areas of the design that are subject to maximum stresses and in danger of fatigue failure. Some of these problems can be addressed or minimized using topology optimisation.

Topology optimisation is a process that evaluates the optimum material distribution for given boundary conditions[16]. Topology optimization is a popular design method for static structures but is still an emerging technology for compliant mechanisms, partially due to the fact that formulating the objective function is still an open research question [17].

Topology optimisation can be done using either the discretized or continuum model approach [18] – visualization of the difference is provided in Figure 5. It is important to note that the continuum model does consist of finite elements, it is how the elements are connected that constitutes the difference between these approaches. In this work we will be focusing on continuum topology optimisation that gives the most versatility and is easily scalable.

Figure 4. Rigid Body Replacement Method.

There are strong advantages of using topology optimisation for designing compliant mechanisms. First is avoidance of the intermediate step of the rigid body mechanism creation and going straight into synthesis of completely new designs. The other benefit is the ability of using general advantages of topology optimisation such as mass reduction, using best material distribution for a given objective, and the potential of easing the design process.

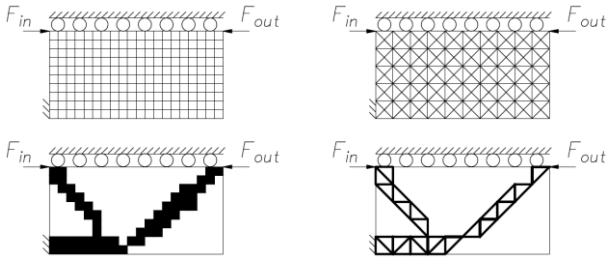

Figure 5. Continuous vs discrete topology optimisation.

5. TOPOLOGY OPTIMISATION OF COMPLIANT MECHANISMS

Commercial CAD software is well suited for optimising structures. The most popular pre-defined problem formulations include:

- best stiffness to weight ratio
- minimize the maximum displacement/minimize compliance
- minimize mass/volume with displacement constraint
- minimize mass/volume with safety factor constraint
- maximize stiffness with mass target

Some tools, e.g. COMSOL and HyperWorks, provide more flexibility for specific problems. The most freedom for the design of compliant mechanisms by topology

optimization currently is made available using MATLAB codes. The codes used to present topologies in this work utilize continuous topology optimisation in 2D. The MATLAB implementations for 3D topology optimisation are also available in the literature [19], [20].

5.1 Problem formulation

Basic formulations of the structural topology optimisation that were mentioned above and are used for designing static structures are quite intuitive. There are also numerous formulations of the objective function for compliant mechanisms available in the literature [17]. Compliant mechanisms need enough flexibility to support the desired kinematic behaviour but should also have enough stiffness to withstand external loads. The most popular interpretations of this problem use strain energy (SE), mutual potential energy (MPE) or the combination of SE and MPE written as a function [17]. This paper focuses on presenting topologies obtained by three MATLAB codes that use the same objective function formulation. The codes are:

i. topm (based on 88 lines code [21] or 99 lines code [22])
ii. the compliant mechanisms version of 188 lines code [23] obtained directly from the authors of the code
iii. Sequential Element Rejection and Admission (SERA) [24] for compliant mechanisms

There are numerous other implementations of topology optimisation scripts in MTLAB available in the literature. Some of them also cover 3D problems [19], [20] but here we will only focus on 2D examples.

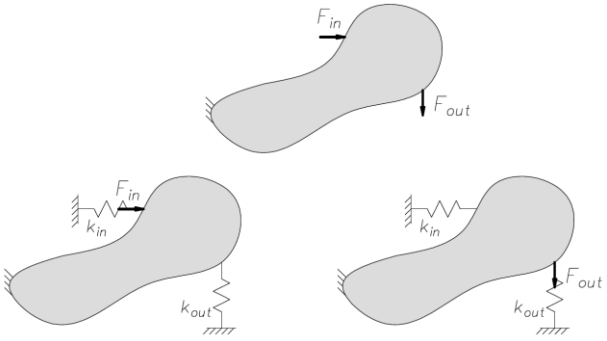

Figure 6. Top: desired problem formulation, bottom left: input force setup for FEM, bottom right: output dummy load for second FEM setup.

The physical representation of the model that is used in the codes under consideration is shown in Figure 6. The figure presents the design domain in grey and the boundary conditions that are attached to it. The top drawing shows the desired behaviour of the mechanism – the input force causes an output force. This is split into two loading cases. The first one with the input force F_{in} applied at the input node, and the second one with unit load applied at the expected output ($F_{out} = 1$). The model also includes two springs: k_{in} attached at the input node and k_{out} attached at the expected output node in both models. Furthermore, any fixed nodes or restricted degrees of freedom need to be defined. The objective function is expressed as mutual potential energy (MPE) that is described in the literature as a functional expression of the output deformation [17]. For all the codes mentioned here the constraint is a volume fraction specified by user. The differences between the codes will be discussed in the subsection 5.2. Nevertheless, they all share the formulation as presented in the Figure 6.

5.2 MATLAB codes

Topm or 99/88 lines script is a Solid Isotropic Material with Penalization (SIMP) method. It is a grid representation approach of continuum topology optimisation. The topologies presented in this work were obtained from the version of the code that utilizes the Optimality Criteria, but it can also be used with the Methods of Moving Asymptotes. The design domain is divided into square elements that are non-binary - meaning they can have values that are fractions of the properties of the solid material (e.g. fraction of density or Young's modulus). At the beginning of the code each element is assigned a value of expected global volume fraction that can be interpreted as intermediate density. This means that for the desired volume fraction of e.g. 0.5 in the first initialization, each element in the design domain will have a density equal to 0.5. The material properties for each element are represented as density raised to a power of penalty times the material properties of solid element [22]. The Young's modulus of each element can then be written as follows:

$$E_e(x_e) = E_{min} + x_e^p (E_0 - E_{min})$$

where x_e is a density of material in the element e ($x_e \in [0, 1]$), E_0 is the stiffness of the material, E_{min} is a very low stiffness assigned to void regions, and p is a penalty [21]. The penalty is responsible for promoting the element densities to move to one of the extremes - empty or full material representation as the intermediate (grey) areas are to be avoided in the final design. At the end of the optimisation some grey elements may still be present especially at the edges of the topology. This may be acceptable for the composite designs, but for most single material problems black-and-white final topologies are desired as grey elements in the SIMP formulation have intermediate densities and Young's modulus. The authors of the 99/88 lines code suggest considering this material representation as composite materials [16]. In the code there is also a filtering technique that looks into the sensitivities of the objective function with respect to the element densities in the radius r_{min} [21]. In other words, sensitivity is a derivative of the objective function with respect to the element density. The parameter r_{min} is the radius inside of which the sensitivity of the central element is based on a weighted average of the sensitivities of its neighbours.

SERA method is an evolutionary structural optimization (ESO) method that uses the Optimality Criteria approach. It belongs to grid representation methods of topology optimisation. More specifically it is a bidirectional version of ESO (BESO). The elements in the design domain can be removed from it but then can also come back in the optimisation process. In contrast to the 99/88 line code, SERA does not have grey elements with intermediate densities. It operates on two lists of elements: full and void elements without any intermediate states [25]. SERA does not assign any penalties because the existence of aforementioned lists of void and full elements remove the problem of grey areas. SERA also utilizes filtering with r_{min}. Sensitivity of each element is based on a weighted average of the sensitivities of its neighbours [25].

The MMC188 code from Zhang et. al. [23] utilises Moving Morphable Components (MMC), which is a geometric representation method of topology optimisation. The code for optimising static structures was published for research purposes [23]. For the purposes of this work, the version for compliant mechanisms was directly requested and obtained from the authors of the code. The MATLAB script uses two external functions written by Krister Svanberg: 'subsolv' and 'mmasub' to utilise the Method of Moving Asymptotes. In the first iteration of optimisation process the design domain is filled with the pre-defined components. The distribution and the shape of those components can be changed in one of the arguments of the MMC188 function. During the optimisation, the components can move inside of the design domain as well as change their shape and orientation. In this method there is no problem with any intermediate elements and each component represents a full density material with well-defined edges.

5.3 Force inverter example

In this section an example of mechanisms obtained with the MATLAB codes will be presented. All codes were run with a problem setup characteristic of a force inverter mechanism provided in Figure 7. Only the bottom half of the inverter has been modelled. The mechanism requires input force from the left, and it is fixed in the top left and bottom left corners. The expected output force (and displacement) is located on the right in the direction that is opposite to the direction of the input force.

The material properties have been set as: Poisson's ratio equal to 0.35 and Young's modulus equal to 2.93 GPa. This represents nylon 6/6. The size considered to be the design domain is 100 x 50 mm represented by 200 x 100 elements. The input force was set to 10 N and the spring stiffnesses to 330 N/mm (output and input springs are identical) and their value has been chosen based on the literature that suggests looking into the stiffness value of the full design domain with fixed output [26].

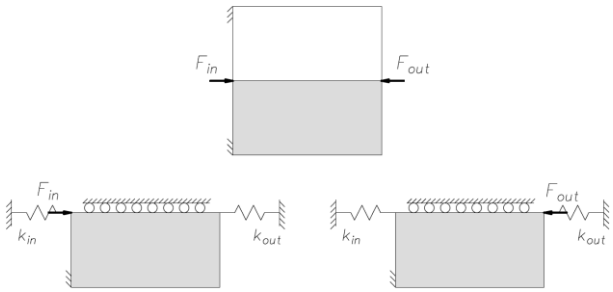

Figure 7. Force inverter problem.

The top 99 lines code [22] was adapted to be used with compliant mechanisms according to Bendsoe [16]. The exact code arguments are specified in Table 1. The mesh size and volume fraction are the same for all examples: mesh consisting of 200 x 100 elements and volume fraction 0.3. The differences lie in the filtering radius and the penalty that is used as a power in the material properties. Explanation of the power impact is available in the literature and it is recommended to use powers above 3 [22]. The SERA code [25] outcomes are presented for a version of code staring with void and full design domains. For the SERA code, two values of filtering radius have been tested – 1.5 and 3. To improve the convergence, the smoothing ratio (SR) parameter was adjusted from the original value of 1.3 to 1.5. MMC code [23] was run with different size and distribution of initial elements in the design domain, see Table 1.

Table 1. Comparison between different codes and parameters.

Top 99 lines	penalty=3, r_{min}=1.5	penalty=4, r_{min}=1.5
	penalty=3, r_{min}=3	penalty=3, r_{min}=3
SERA	r_{min}=1.5, full starting domain	r_{min}=3, full starting domain
	r_{min}=1.5, void starting domain	r_{min}=3, void starting domain
MMC	Distribution 1	Distribution 3
	Distribution 2	Distribution 4

Table 1 presents topologies of a compliant force inverter problem obtained by the aforementioned MATLAB codes. On the left of each final topology there is a starting design domain for which white represents void, black implies full material, and grey is intermediate material state. Crucial code parameters that are input to the function are specified in the table. Topm features different values of filtering radius and penalty. The

SERA code is presented for two values of filtering radius and with the starting design domain being full or empty. MMC code application differs in initial distribution of staring elements in the design domain.

Tables 2, 3 and 4 present outcomes of finite element analysis (FEA) of selected examples from Table 1. The input force of 10 N has been used as in the topology optimisation process but also additional analyses for forces of 2.5 and 5 N are also presented. The software used was Abaqus. The 'Nlgeom' setting was turned on to account for nonlinear behaviour resulting from large deflections in the model. The plots in the tables show the distribution of stress where red represents the maximum stress value for each model. The dark grey topologies in the background are undeformed models while the stress distribution is presented on the deformed half-inverter with deformation scale equal to 1. The numerical data in the tables show the output displacement value and maximum stress for each loading scenario. As the results show, the kinematic behaviour of the mechanism is as desired. It is also evident that some loading scenarios result in maximum stress exceeding the Yield strength for nylon 6/6 which is around 90 MPa. This implies that plastic deformation would occur in this mechanism if manufactured using nylon 6/6.

Table 2. Design verification for Topm, penalty=3, r_{min}=1.5.

Deformation and stress distribution at 10 N.		
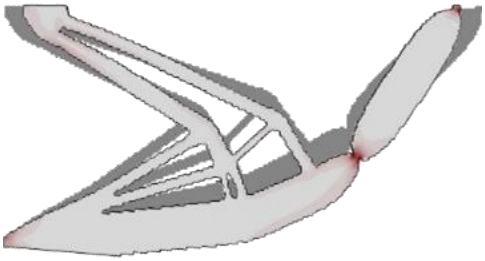		
Force [N]	Displacement [mm]	Max. Stress [MPa]
10	5.1	215
5	2.2	132
2.5	1.1	69

Table 3. Design verification for SERA, r_{min}=1.5, full starting domain.

Deformation and stress distribution at 10 N.		
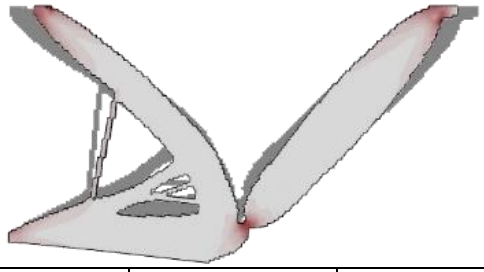		
Force [N]	Displacement [mm]	Max. Stress [MPa]
10	1.0	174
5	2.3	92
2.5	4.8	47

Table 4. Design verification for MMC, topology with initial distribution 1 (shown in Table 1).

Deformation and stress distribution at 10 N.		
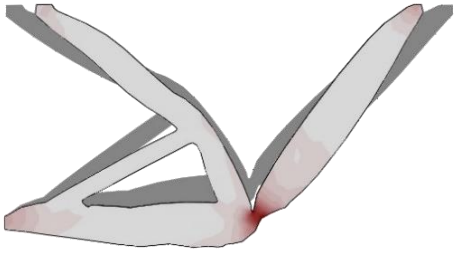		
Force [N]	Displacement [mm]	Max. Stress [MPa]
10	1.1	177
5	2.9	86
2.5	7.2	42

6. FINAL CONCLUSIONS

The topologies presented here were obtained using MATLAB codes for 2D applications of compliant mechanisms. In this work we demonstrated that topology optimisation of complaint mechanisms is possible using the codes available in the literature. Compared to commercial software, the MATLAB codes give the user a great deal of flexibility and access to the optimization parameters. The user can adjust the code to improve convergence or build an objective function tailored to specific needs. Using FEM the kinematic performance and stress distribution were assessed. All designs evaluated had the expected direction of the output displacement but their maximum stress for given input force of 10 N would cause some plastic deformations. Smaller forces would allow staying in safer stress levels but would also result in lower deformations. This clearly demonstrates that selection of the material for a specific application and size with respect to the expected displacements play an important role for compliant mechanisms. The topologies obtained here for the basic codes present quite localized compliance. It is also possible to employ additional filtering techniques or apply different formulations to obtain better distribution of stress and compliance. Nevertheless, this paper shows that topology optimisation can be used as a design aid to obtain mechanisms topologies that are friction free and together with careful material selection could solve some of the Lunar dust related problems.

ACKNOWLEDGEMENTS

This project is funded by the European Space Agency through ExPeRT - Exploration Preparation, Research and Technology program. The authors would like to thank ESA for supporting this research. We gratefully acknowledge the assistance of Antonio Fortunato in supporting the development of ESA – University of Glasgow collaboration and in providing the opportunity to develop the work presented. We would also like to express gratitude to numerous researchers who make their MATLAB scripts public and accessible to us.

REFERENCES

[1] J. E. Colwell, S. Batiste, M. Horányi, S. Robertson, and S. Sture, "Lunar surface: Dust dynamics and regolith mechanics," *Reviews of Geophysics*, vol. 45, no. 2, pp. 1–26, 2007.

[2] J. R. Gaier, "The Effects of Lunar Dust on EVA Systems During the Apollo Missions," *Nasa/Tm-2005-213610/Rev1*, no. March, 2007.

[3] L. B., "Apollo 17 preliminary science report," *Scientific and Technical Information Office NASA*, 1973.

[4] International Space Exploration Coordination Group / Technology Working Group, "GLOBAL EXPLORATION ROADMAP CRITICAL TECHNOLOGY NEEDS," 2019.

[5] S. Pirrotta, D. Lefebvre, M. W. Co-chair, H. Wong, J. Buffington, and J. J. Gaier, "DUST MITIGATION GAP ASSESSMENT REPORT," 2016.

[6] J. E. Colwell, S. R. Robertson, M. Horányi, X. Wang, A. Poppe, and P. Wheeler, "Lunar dust levitation," *Journal of Aerospace Engineering*, vol. 22, no. 1, pp. 2–9, 2009.

[7] J. R. Gaier, "Regolith activation on the lunar surface and its ground test simulation," *SAE Technical Papers*, no. April, 2009.

[8] T. J. Stubbs, J. S. Halekas, W. M. Farrell, and R. R. Vondrak, "Lunar surface charging: A global perspective using lunar prospector data," *ESA - Workshop on Dust in Planetary Systems*, pp. 181–184, 2007.

[9] T. L. Jackson, W. M. Farrell, and M. I. Zimmerman, "Rover wheel charging on the lunar surface," *Advances in Space Research*, 2015.

[10] L. L. Howell, S. P. Magleby, and B. M. Olsen, *Handbook of Compliant Mechanisms*, no. 2013. 2019.

[11] L. Zhao, X. Yu, P. Li, and Y. Qiao, "High-precision compliant mechanism for lens XY micro-adjustment," *Review of Scientific Instruments*, vol. 91, no. 3, 2020.

[12] J. Pinskier, B. Shirinzadeh, M. Ghafarian, T. K. Das, A. Al-Jodah, and R. Nowell, "Topology optimization of stiffness constrained flexure-hinges for precision and range maximization," *Mechanism and Machine Theory*, vol. 150, p. 103874, 2020.

[13] L. Liu, S. Bi, Q. Yang, and Y. Wang, "Design and experiment of generalized triple-cross-spring flexure pivots applied to the ultra-precision instruments," *Review of Scientific Instruments*, vol. 85, no. 10, 2014.

[14] L. L. Howell, *Compliant Mechanisms*. Wiley, 2001.

[15] R. Two, O. Performances, X. Zhang, and B. Zhu, *Topology optimization of compliant mechanisms*. 2018.

[16] O. S. Martin Philip Bendsoe, *Topology Optimization: Theory, Methods, and Applications*, vol. 89, no. 9. 2003.

[17] A. Saxena and G. K. Ananthasuresh, "On an optimal property of compliant topologies," pp. 36–49, 2000.

[18] Y. Saadlaoui, J. L. Milan, J. M. Rossi, and P. Chabrand, "Topology optimization and additive manufacturing: Comparison of conception methods using industrial codes," *Journal of Manufacturing Systems*, vol. 43, no. October, pp. 178–186, 2017.

[19] R. Ansola, E. Veguería, C. Alonso, and O. M. Querin, "Topology optimization of 3D compliant actuators by a sequential element rejection and admission method," *IOP Conference Series: Materials Science and Engineering*, vol. 108, no. 1, 2016.

[20] F. Ferrari and O. Sigmund, "A new generation 99 line Matlab code for compliance topology optimization and its extension to 3D," *Structural and Multidisciplinary Optimization*, vol. 62, no. 4, pp. 2211–2228, 2020.

[21] E. Andreassen, A. Clausen, M. Schevenels, B. S. Lazarov, and O. Sigmund, "Efficient topology optimization in MATLAB using 88 lines of code," *Structural and Multidisciplinary Optimization*, vol. 43, no. 1, pp. 1–16, 2011.

[22] O. Sigmund, "A 99 line topology optimization code written in matlab," *Structural and Multidisciplinary Optimization*, vol. 21, no. 2, pp. 120–127, 2001.

[23] W. Zhang, J. Yuan, J. Zhang, and X. Guo, "A new topology optimization approach based on Moving Morphable Components (MMC) and the ersatz material model," *Structural and Multidisciplinary Optimization*, pp. 1243–1260, 2016.

[24] C. Alonso and O. M. Querin, "A Sequential Element Rejection and Admission (SERA) method for compliant mechanisms design," pp. 795–807, 2013.

[25] R. A. Loyola, O. M. Querin, A. G. Jiménez, and C. A. Gordoa, "A sequential element rejection and admission (SERA) topology optimization code written in Matlab," pp. 1297–1310, 2018.

[26] S. Rahmatalla and C. C. Swan, "Sparse monolithic compliant mechanisms using continuum structural topology optimization," no. August 2004, pp. 1579–1605, 2005.